powders

MDPI

Project Report

Highly Permeable, Electrically Switchable Filter for Multidimensional Sorting of Suspended Particles

Laura Weirauch [1], Jasper Giesler [1], Georg R. Pesch [2], Michael Baune [1,3] and Jorg Thöming [1,3,*]

[1] Chemical Process Engineering, Faculty of Production Engineering, University of Bremen, 28359 Bremen, Germany
[2] School of Chemical and Bioprocess Engineering, University College Dublin, D04 V1W8 Dublin, Ireland
[3] Center for Environmental Research and Sustainable Technology (UFT), University of Bremen, 28359 Bremen, Germany
* Correspondence: thoeming@uni-bremen.de

Abstract: The creation of highly specific particle systems in the nano- and micrometer size range is a challenging task. The demand for particle systems with narrowly distributed properties is increasing in many applications, especially for use in high-tech products. Conventional separation techniques often reach their limits in the micrometer size range or become (labor-)intensive, which makes them economically or ecologically unsustainable. In addition, sorting based on several properties is rarely feasible in just one separator. Dielectrophoretic processes can be a viable option for complex sorting tasks like this, given their ability to address several particle properties and their high degree of selectivity. In this paper, we summarize the progress of a project in which the capability of dielectrophoretic methods for multidimensional sorting of microparticles was investigated. We were able to develop an operation mode for multidimensional sorting of microparticles using dielectrophoresis as well as a scalable electrically switchable filter. This creates a basis for high-throughput and multi-target sorting of technical microparticles using dielectrophoretic processes.

Keywords: dielectrophoresis; filtration; selective separation; multidimensional; high-throughput; microparticles; millifluidics

Citation: Weirauch, L.; Giesler, J.; Pesch, G.R.; Baune, M.; Thöming, J. Highly Permeable, Electrically Switchable Filter for Multidimensional Sorting of Suspended Particles. *Powders* **2024**, *3*, 574–593. https://doi.org/10.3390/powders3040030

Academic Editor: Sergiy Antonyuk

Received: 28 August 2024
Revised: 23 October 2024
Accepted: 20 November 2024
Published: 25 November 2024

1. Introduction

To fulfill a function, e.g., in high-tech products like energy storage components [1] or sensors [2], particles often have to be specific in more than one property. While several studies investigate size-based sorting of microparticles, other properties such as sorting based on shape or surface properties, are less often considered [3]. We refer to simultaneous sorting based on several particle properties as multidimensional separation [4]. Such a separation can usually only be realized with multiple interconnected or label-based processes [5]. Current research on this topic is reflected in the priority program SPP 2045 "MehrDimPart—highly specific multidimensional fractionation of fine particles with technical relevance" of the German Research Foundation. The aim of the priority program was to develop processes capable of creating highly specific microparticle systems through multidimensional sorting. We summarize one of its projects here, C1 (TH 893/20-1 and TH 893/20-2). In this project, we investigate whether dielectrophoresis enables the sorting of suspended particles based on multiple properties in one pass of a device.

Dielectrophoresis (DEP) is the movement of polarizable particles in an inhomogeneous electric field. The time-averaged DEP force on a prolate ellipsoidal particle can be approximated by [6]

$$\langle \vec{F}_{\mathrm{DEP,pr},i} \rangle = \pi a_j a_k^2 \varepsilon_{\mathrm{m}} \mathrm{Re}(\tilde{f}_{\mathrm{CM},i}) \nabla |\vec{E}|^2 \,. \quad (1)$$

The force depends on the particle volume with the radii of the half axis $a_j \geq a_k = a_l$, dielectric properties of the medium and particle (permittivity ε_{m} and $\tilde{f}_{\mathrm{CM},i}$), and the gradient

of the electric field squared. Here, $|\vec{E}|$ is the amplitude of the electric field given in V m^{-1}. $\mathrm{Re}(\tilde{f}_{\mathrm{CM},i})$ is the real part of the so-called Clausius–Mossotti factor [6,7]

$$\mathrm{Re}(\tilde{f}_{\mathrm{CM},i}) = \mathrm{Re}\left(\frac{\tilde{\varepsilon}_{\mathrm{p},a_i} - \tilde{\varepsilon}_{\mathrm{m}}}{3(\tilde{\varepsilon}_{\mathrm{m}} + (\tilde{\varepsilon}_{\mathrm{p},a_i} - \tilde{\varepsilon}_{\mathrm{m}})L_{a_i})}\right) \tag{2}$$

giving the relative polarizability of a particle (index p) in its surrounding medium (index m). For a prolate ellipsoid, it differs for each half-axis i, as the depolarization factor L_{a_i} and the particle's complex permittivity $\tilde{\varepsilon}_{\mathrm{p},a_i}$ vary depending on the orientation of the particle in the electric field. L_{a_i} quantifies the reduction in the electric field inside the polarized particle relative to the external field caused by induced polarization charges on the particle's surface [8]. The complex permittivity $\tilde{\varepsilon}$ for a dielectric with losses, what both particle and medium are considered to be, includes the permittivity $\varepsilon = \varepsilon_0\varepsilon_{\mathrm{r}}$ and conductivity σ of the material

$$\tilde{\varepsilon} = \varepsilon_0\varepsilon_{\mathrm{r}} - \frac{j\sigma}{\omega}\,. \tag{3}$$

This results in a dependence of the DEP force on the frequency of the applied field f with ω being the angular frequency ($\omega = 2\pi f$). The particle conductivity along each axis of a prolate ellipsoidal particle can be approximated by [9]

$$\sigma_{\mathrm{p},a_j} = \sigma_{\mathrm{p,bulk}} + \frac{2K_{\mathrm{S}}}{a_k} \qquad \sigma_{\mathrm{p},a_k} = \sigma_{\mathrm{p,bulk}} + \frac{(a_j + a_k)K_{\mathrm{S}}}{a_j a_k}\,. \tag{4}$$

Here, K_{S} is the surface conductance of the particle which is caused by the formation of an electrical double layer around the particle in an aqueous solution. For materials with low bulk conductivity $\sigma_{\mathrm{p,bulk}}$, such as polystyrene (PS) which is used in this project, the contribution of surface conductivity to the overall particle conductivity can be predominant [10,11]. For spherical particles, with $a_j = a_k = a_l = r$, the depolarization factor becomes $\frac{1}{3}$, and Equations (1), (2), and (4) simplify to the familiar DEP equations for spherical particles.

A distinctive feature of the DEP force is that it can change direction depending on the properties of the medium, the particle, and the frequency of the applied field. This is reflected in the sign of $\mathrm{Re}(\tilde{f}_{\mathrm{CM},i})$ and can be used to control which particles are retained in a DEP device. When $\mathrm{Re}(\tilde{f}_{\mathrm{CM},i})$ is positive, the force acts in the direction of the electric field gradient towards field maxima, which is called positive DEP (pDEP). Conversely, when $\mathrm{Re}(\tilde{f}_{\mathrm{CM},i})$ is negative, the force points against the gradient towards local field minima, which is called negative DEP (nDEP). Many particles, depending on their properties, have a transition point from pDEP to nDEP at a specific frequency and medium conductivity, commonly referred to as crossover.

In this project, field inhomogeneities are generated by inserting an insulating structure in an originally nearly homogeneous electric field between two electrodes. This structure disturbs the electric field. The concept is called insulator-based dielectrophoresis (iDEP). Retention in a device with insulating field disturbers by DEP forces can occur when particles are attracted to the insulating structures by pDEP forces. Here, field maxima are located parallel to the electric field at the field disturber edges, which serve as trapping spots (Figure 1, for photos of trapping in real DEP channels—see Figure A3). However, retention can also occur if the particles experience strong nDEP forces. In such instances, the particles may be strongly repelled by the field maxima or trapped in local minima, resulting in their retention. The insulating structure thus serves as a filter in which the particles are retained via DEP if an electric field is applied. The pores of the insulating structure can be significantly larger than the particles, making it highly permeable and enabling the filter to be electrically switchable. Negative DEP forces on the particles are generally weaker than the pDEP forces, as the field gradients around field minima are usually much lower compared to field gradients around field maxima. Thus, pDEP filtering is usually more efficient and is used in this project. Particles can be selectively trapped in [12–14] and selectively remobilized out of DEP filters depending on their properties. The latter can be

realized by reducing the voltage until the force acting on one particle species is too small to retain it (below the minimum trapping voltage). This has been previously shown in several DEP studies (e.g., refs. [15,16]) and in experiments during this project [17]. If the particle types experience a similar magnitude of the DEP force, e.g., because they have a similar particle volume, a sorting is challenging or even impossible.

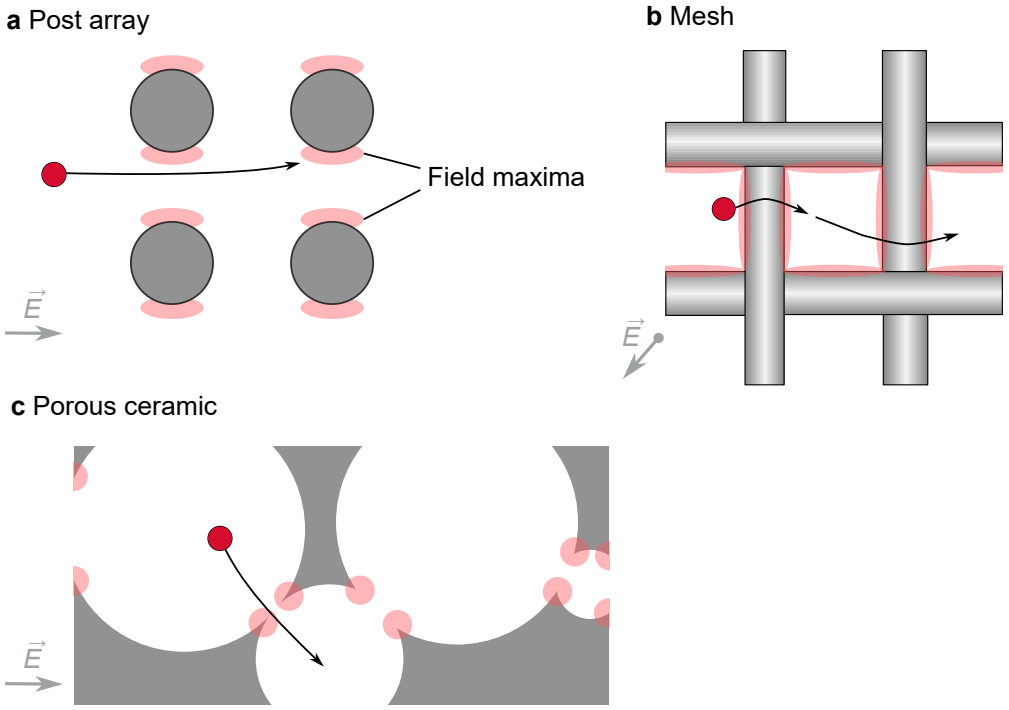

Figure 1. Different insulating material geometries used for DEP filters in this project (top view). The flow direction is from left to right, and the direction of the electric field $\vec{E}$ is indicated by an arrow. Particles (illustrated by red circles) can be retained by positive DEP at the field maxima shown for a post array (**a**), a mesh material (**b**), and a porous ceramic filter matrix (**c**).

In this project, we exploited the fact that particles show different variations of $\mathrm{Re}(\tilde{f}_{\mathrm{CM},i})$ over the frequency of the applied electric field. By changing the frequency of the electric field, both the magnitude and the direction of the force acting on a particle can be changed and differences in DEP behavior between two particle types enhanced. In this project, we were the first to investigate if the specific crossover of a particle with distinct properties can be used to sort particles based on multiple characteristics. A combination of selective trapping and subsequent selective remobilization of single particle types was investigated for achieving this in one pass of a DEP filter. Furthermore, to enable the use of this sorting technique for technical particles it should be realizable in a scalable device. One problem why DEP processes have so far hardly been used commercially and almost exclusively in the biomedical field [18] is their lack of scalability while maintaining high selectivity. Most methods are developed in microfluidic setups that enable high selectivities but are limited to volume flows in the microliter to milliliter range [19]. There are a few approaches to overcome this throughput limitation, such as the use of electrically insulating packed beds or porous structures between widely spaced electrodes in macroscopic devices [20–23]. The drawback of these concepts is that such devices are unlikely to reach the selectivity of state-of-the-art microfluidic DEP or electrokinetic separators [24]. In this project, regular field disturbing structures (meshes) are used to increase selectivity and thus enable multidimensional sorting.

Detailed results of the project have already been published elsewhere [17,25,26]. In refs. [17,25], a model particle system based on polystyrene was established with particles differing in only one property compared to a reference particle, e.g., the shape or the

surface material. The investigations intended to improve the general understanding of DEP separation based on different particle characteristics by specifically investigating the influence of individual particle properties. Furthermore, a scalable DEP filter design was developed [25]. The mesh-based DEP filter with regular field-disturbing structures allowed us to increase the throughput while maintaining high selectivity. Finally, multidimensional sorting in the scalable filter was demonstrated [26]. This manuscript summarizes the developed methods and results, discusses the outcome of this project, and provides an outlook for future research.

2. Materials and Methods

2.1. Particle System

To simplify the process development, we conducted all our experiments with model particles based on fluorescent polystyrene microparticles (microParticles GmbH, Berlin, Germany and Polysciences Europe GmbH, Hirschberg, Germany). PS particles are commonly used as standard model particles in research but also have practical applications, such as serving as drug carriers [27]. In this stage of process development, using real particle systems, such as black mass from battery recycling, was not favorable due to the absence of online monitoring systems, the lack of straightforward evaluation methods, and the wide variation in properties (e.g., size and material heterogeneity). The fluorescence of the model particles enabled online measurement, straightforward evaluation, and visualization of particle movement in the DEP channels. The initial properties of PS particles are standardized and monodisperse, and various methods exist for their modification. This makes them well suited for studying multidimensional sorting. In this project, we created a model particle system with each particle species differing from a base particle in only one property at a time. For example, when varying the particle shape, the volume and material remained as constant as possible. The influence of size, shape, and material (surface coating) was examined. The possibility to separate each particle modification from unmodified particles was first tested in microchannels, on a scale established in DEP [17,25]. This ensured that the individual particles of the particle system were suitable for studying material- and shape-dependent separation.

Material variation

To investigate the influence of the particles surface material, the particles were modified using a gold coating process (based on [28–30]). The procedure was adapted to maintain the base fluorescence of the modified particles. For this, the particles are seeded with gold nanoparticles and then coated by a reduction reaction of gold (I) sodium thiosulfate with ascorbic acid (for details on the process, see ref. [17]). The coating facilitates the investigation of the surface material's influence at a smaller density difference compared to solid metal spheres. The dielectrophoretic behavior of coated particles (Figure 2a) was shown to agree well with the theoretical behavior of solid conducting spheres in the frequency range used in this project [30].

Shape variation

To investigate the shape influence, a stretching process (based on [31]) was used. The PS particles were deformed into an ellipsoidal shape (Figure 2b) without losing their fluorescence. The particles are suspended in an aqueous polyvinyl alcohol (PVA, Parteck COAT, Merck KGaA, Darmstadt, Germany) solution. When cooling this suspension, a solid film forms that embeds the particles in a PVA matrix. Subsequently, the film is stretched in a heated oil bath. During the stretching, both the particles and film are elongated. Afterwards, the particles can be recovered by dissolving the film in water. Again, the parameters of the process were adjusted to use fluorescent particles in this project (for details see ref. [25]). The process changes the shape of the particles without changing their volume. In the DEP literature, different materials (e.g., different cell types) were often used to examine shape-selective separation [32,33]. The use of the stretching method, on the other hand, allows us to consider the purely geometric aspect of the particle shape.

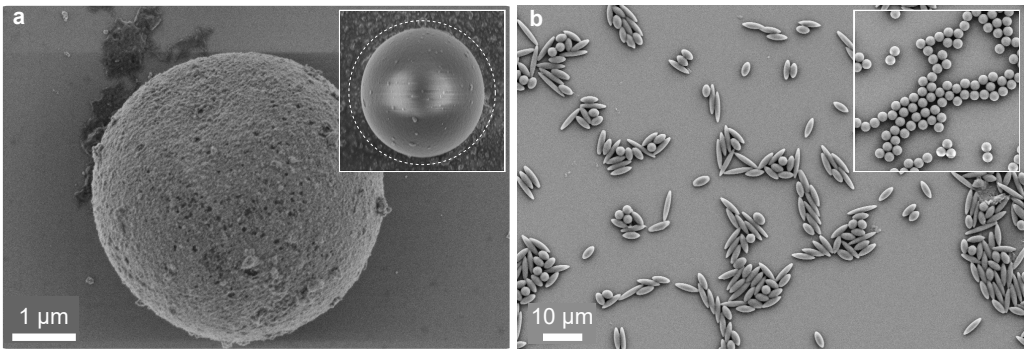

Figure 2. SEM images of the modified particles used in this project. (**a**) Gold-coated 4.5 µm PS particle. An almost closed layer of about 200 nm thickness was formed on the particle surface. Through this gold layer the fluorescence still can be detected. Inset: Size comparison between a coated (dashed line) and uncoated particle (based on ref. [17]). (**b**) Ellipsoidal PS particles. Their shape has been modified by a stretching process. Inset: Treated PS particles without stretching (based on ref. [25]).

Size variation

To investigate the volume's influence, differently sized PS particles were used. To exclude the possibility that the embedding in PVA during the stretching process limits the comparability, spherical PS particles were treated like the ellipsoids (embedded in PVA, etc.), apart from the stretching process itself. These are referred to as "treated" in the following sections.

2.2. Experimental Setup and Procedure

During this project, a total of three different DEP setups were utilized (see Figure 3). As a starting point, we used a microfluidic DEP method with an electro-osmotic-driven flow (DC-iEK, Figure 3a), which is established in the literature and thus acted as a well-defined basis for our experiments. Subsequently, a pressure-driven microfluidic method more suitable for non-biological particles with higher sample throughputs was used (AC-iDEP, Figure 3b). Finally, to show the applicability of our method at high throughput, a third and scalable version of a DEP filter was developed (mesh-based macrochannel, Figure 3c). The following is a brief introduction to the DEP setups and associated experimental procedures. Details like model types of the equipment and manufacturers can be found in refs. [17,25,26]. For all experiments, particles were suspended in a mixture of ultrapure water, Tween20 to reduce particle–wall interactions, potassium hydroxide to adjust pH, and potassium chloride to adjust the electrical conductivity to the desired value. The medium conductivity will be specified in each section.

2.2.1. Microchannels

DC-iEK

To investigate the influence of a gold coating on the particle behavior, a standard technique called DC-iEK was used. DC-iEK is a highly selective DEP method widely used in the biomedical field (refs. [34,35]). Here, an electrokinetic (EK) motion of particles, caused by electro-osmosis (EO) and electrophoresis (EP), is used to carry particles through a microchannel with a post array. Both phenomena are based on the attraction of opposite charges in a DC electric field, whereby in the case of EO the fluid is set in a directed motion, and in the case of EP, the force acts directly on the particle. For negatively charged particles in polydimethylsiloxane (PDMS) channels, like in this study, EP counteracts the particle motion caused by EO. Particles can be retained in the post array if (linear and non-linear) EP and nDEP overcome the EO motion of the particle. Depending on the particle's properties, nDEP and non-linear EP can result in the particle being strongly repelled by the field maxima between the posts, preventing it from being able to pass. As the phenomena scale

with the electric field strength, there is a minimum voltage at which each particle type starts to be trapped (minimum trapping voltage).

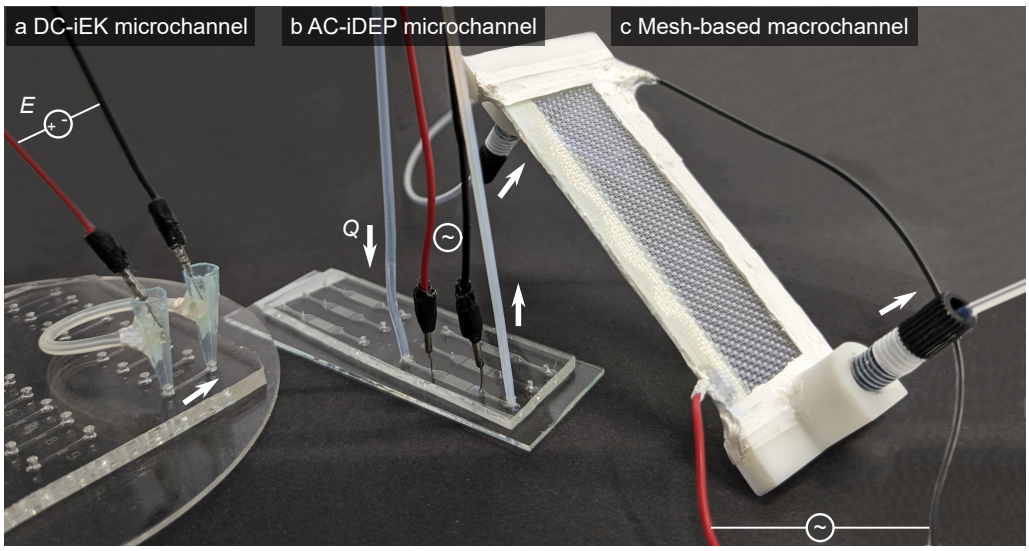

Figure 3. Photography of the DEP channels used in this project. (**a**) DC-iEK microchannel with an electro-osmotic-driven flow used as a benchmark DEP method. A particle sample comprising a few µL can be processed, and an electric field E above 1 kV_{DC} cm^{-1} is needed for retaining the particles. (**b**) AC-iDEP microchannel with a pressure-driven flow. Volume flow Q of around 0.1 mL h^{-1} can be handled, and an electric field E around 2.5 kV_{pp} cm^{-1} is used for particle trapping. (**c**) Mesh-based iDEP macrochannel with a pressure-driven flow. Volume flow Q of around 120 mL h^{-1} is used, and an electric field E around 2.4 kV_{pp} cm^{-1} is needed for particle trapping. The values given here refer to the retention of PS-based particles and medium properties used in this study.

Insulator-based microchannels made out of PDMS were used for the DC-iEK method (for a sketch, see Figure A2a). They were fabricated with a standard soft lithography technique. The channels contained a 14 by 4 array of cylindrical insulating posts with a diameter of 200 µm and spacing of 20 µm at the channel center for particle separation. Two pipette tips serve as liquid reservoirs at the channel inlet and outlet. The electric field in the microchannels was applied with two platinum wire electrodes immersed in the reservoirs. We modified the standard DC-iEK channels by connecting the two reservoirs with a silicone tube to compensate for pressure differences between both of them. A backpressure builds up over time when the fluid is pumped to one side of the channel by EO and changes the reservoir filling level of the in- and outlet, which gradually reduces the required trapping voltage. This behavior made reproducible iEK trapping difficult in our experiments. Imaging of the microchannel was carried out with an inverted microscope.

For separation experiments, 1 µL of a particles mixture, containing 4×10^6 particles mL^{-1}, was injected into the channel. A high DC voltage was applied (above the minimum voltages required for trapping both particle types) until all particles injected into the system were retained in the post array. Then, the voltage was reduced to a value between and subsequently below the minimum trapping voltages of the two particle types. This first reduction releases all particles of one type (with a higher minimum trapping voltage) and then, at a lower voltage, all particles of the second type. Videos were recorded at the channel outlet to detect particle release. As a quantification of separation success, the normalized purity Equation (A3) and yield Equation (A2) were considered. For this purpose, the fluorescence intensities were determined for the different fluorescence colors of the particles types from the videos, and it was assumed that the fluorescence intensity I is proportional to the particle concentration c.

AC-iDEP

The influence of the particle shape was investigated using an AC-iDEP method. In contrast to DC-iEK, the AC-iDEP method used here uses a pressure-driven flow instead of EO to transport the particles to trapping spots. The particles will be separated by trapping target particles with a strong pDEP force on the post array, while non-target particles showing nDEP or weak pDEP travel through the filter unaffected. To retain and hold particles in trapping spots out of a pressure-driven flow, the DEP force must overcome hydrodynamic forces, Brownian motion, and diffusion.

The microchannels used for the pressure-driven experiments were also fabricated using a standard soft lithography technique (for a sketch, see Figure A2b). A 10 by 7 post array of cylindrical insulating posts with a diameter of 260 µm and spacing of 100 µm was located in the center of the microchannel. An electric field was applied by using two platinum wire electrodes placed 9 mm apart. The electrodes were inserted into the channel via punched holes in the PDMS substrate. The particle suspension was pumped into the microchannel with a syringe pump. Imaging of the microchannels was carried out with an upright microscope. In this project, the standard straight channel design (e.g., used in ref. [22]) was modified by narrowing the channel before and after the electrodes. In iDEP microchannels, a formation of vortex flows at the millimeter scale around the electrodes is observable, which is assumed to be caused by a combination of nonlinear electrokinetic effects. The origin of this vortex formation could not be clearly identified in this project. However, the effect on the reproducibility of the experiments could be reduced by the aforementioned modification by accelerating the fluid flow near the electrodes and slowing it down in the trapping zone (post array).

Separation experiments in the microchannels were carried out with a binary particle mixture. Each particle type had a concentration of 2.5×10^5 particles mL^{-1}. The particles were trapped in the filter for a few minutes and recovered by switching off the voltage. For each datapoint, three repetitions were made, each with three video recordings. An in-house MATLAB program in combination with the TrackMate Plugin of Fiji was used to evaluate particle trapping in the channel. The trapping efficiency (Equation (A1)) and purity (Equation (A3)) were calculated. In this case, calculating a yield is not meaningful, since no particle sample was separated in these validation experiments; instead, the particle suspension was permanently flushed through the channel.

2.2.2. Mesh-Based Macrochannel

The influence of the particle size and, finally, multidimensional sorting was investigated in a macroscopic setup. The concept for and a prototype of a scalable DEP filter was introduced in one of our previous publications (ref. [25]). The goal was to develop a DEP filter using a regular filter matrix in which high throughputs are possible while maintaining the high selectivity of microfluidic DEP processes. The prototype should at least be able to process a volumetric flow rate of 60 mL h^{-1} to ensure the generation of sufficient sample volumes within a reasonable amount of time and to be comparable to previous DEP filters of our group based on irregular filter structures [23,36]. The minimum throughput makes subsequent analytical procedures (like material analysis) possible, which is particularly valuable for testing particle mixtures in the future that do not emit fluorescence.

The mesh-based DEP filter consists of two conductive indium tin oxide (ITO)-coated glass slides as electrodes, which form the ceiling and bottom of the channel with a distance of 0.7–0.9 mm (Figure 3c; for a sketch, see Figure A2c). For the prototype, the transparency of the ITO electrodes helps to understand the motion of the particles within the filter and visually differentiate nDEP and pDEP trapping. A polypropylene (PP) fabric (open square weave) with a mesh width of 500 µm and a fiber diameter of 340 µm is sandwiched between the electrodes, generating field inhomogeneities. Fluid distributors were 3D-printed and, like the channel sides, sealed with a polymer glue. The fluid flows parallel to the surface of the mesh through its cross-section. The mesh-based approach serves as a direct upscaling

of a post-array-based, pressure-driven microfluidic iDEP channel. Accordingly, particles are captured via pDEP forces on the field disturbers (mesh fibers).

The experimental setup of the mesh-based DEP filter was described in detail in ref. [25]. The fluid flow was generated by a piston pump, and the voltage was supplied by a signal generator connected to a power amplifier. A fluorescence spectrometer setup was used for data acquisition at the channel outlet. The spectrometer setup was assembled of a spectrometer, a light source, a triple band-pass filter, and a flow-through cuvette. Additionally, an inverted microscope and a camera were used to record videos of the inside of the filter. The particle suspensions for the experiments contained a concentration of 2.5×10^5 particles mL^{-1} for each particle type. For mixtures up to three particle types with different fluorescence colors, the fluorescence intensity for each type was determined with a linear unmixing procedure (for details, see ref. [25]). For more than three colors, the deviations between the calculated fluorescence intensity for each type and the observed particle behavior in the filter mesh, as well as in comparison to experiments with only one type of particle present in the suspension, were too high. The main reason for this seemed to be that two similar fluorescent colors had to be chosen for two particle types, as there is only a limited choice of different fluorescent markers available for the particles that also match the used fluorescence filter. Therefore, the trapping efficiency and yield were determined from single-particle-type experiments. The transferability to experiments with particle mixtures was ensured by preliminary experiments. The purity, on the other hand, was determined from experiments with particle mixtures. For this, samples were collected at different times during the experiments, concentrated by centrifugation, and freeze-dried; scanning electron microscopy (SEM) images were taken; and then the samples were analyzed by counting the different particle types.

2.3. Concept of Multidimensional Separation

To separate particles multidimensionally in one pass of a DEP filter, a stepwise change of the frequency of the electric field is used in this project. This exploits the different dependence of the dielectrophoretic behavior of particles with different properties on the frequency. To select suitable frequencies, the K_S value of the particles was estimated and $\mathrm{Re}(\tilde{f}_{CM})$ was calculated for different applied frequencies (Figure 4b). For a multidimensional sorting of four different particle types, for the first step, a sufficiently high voltage U and frequency were chosen, where all particles except one type were showing pDEP (selective trapping step at f_1). During this step, the not-trapped particles are enriched with respect to the other particle types in the outlet flow (Figure 4a, blue particles).

In order to increase the purity of the subsequent remobilized fractions, the feed is changed to a flushing solution without particles. Afterward, the retained particles can be sorted regarding different properties by shifting the frequency to a point, where only one particle type switched to nDEP (selective remobilization steps at f_2 red particles, f_3 green particles), while maintaining voltage U. The last remaining particle type (yellow) can be recovered by switching off the electric field (recovery step). This time-based sorting can be repeated by a periodical injection of a particle mixture into carrier flow.

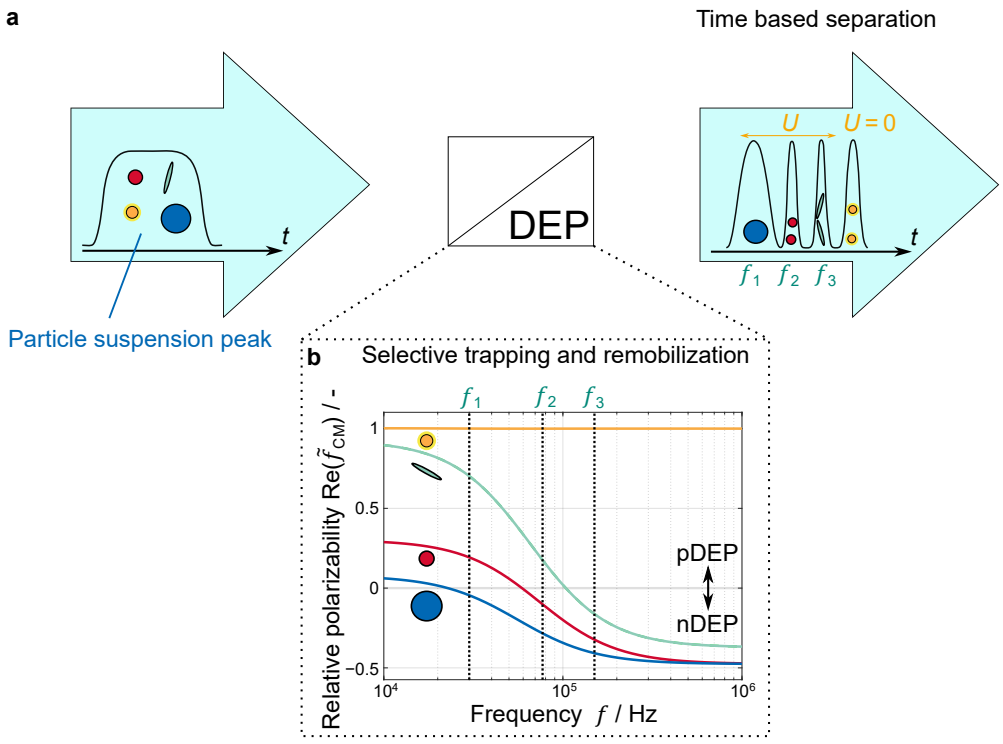

Figure 4. (**a**) Sketch of a batch operation mode of a DEP filter which sorts according to several particle properties (illustrated by differently colored circles or ellipses) in one pass. A particle pulse entering the filter is selectively trapped by DEP. Afterward, the retained particles can be sorted by selectively remobilizing different fractions by adjusting the frequency f of the electric field with voltage U. (**b**) Relative polarizability of the model particle species over the frequency. Example graph for a conductivity of $\sigma_m = 1.5$ µS cm^{-1} and the particles used in Section 3.4.

3. Results and Discussion

3.1. Material-Selective Separation

The separability of gold-coated particles from uncoated particles was first investigated in DC-iEK experiments using 2.4 µm particles (published in ref. [17]). In this way, it can be verified whether the dielectrophoretic properties of the modified particles have been altered enough for separation, and the results provide a benchmark for the scalable procedure developed in this project. The electrokinetic behavior of the particles in the DC-iEK microchannel fits well to the theory as coated particles show lower particle velocities than uncoated particles. This results in lower minimum trapping voltages for the conductively coated particles. At a trapping voltage of 900 V_{DC}, no fluorescence is detected at the microchannel outlet (see dielectropherogram in Figure 5a, first 20 s), which means that both particles are completely retained. The following two-step voltage reduction (300 V_{DC} and 40 V_{DC}) results in two narrow and clearly separated peaks for the uncoated and coated particles. Smaller peaks in the PS particle curve (red) after the second voltage reduction are due to small agglomerates, which are more easily retained due to their size. A normalized purity of 100% ± 0% is obtained for the uncoated PS particles, while for the Au-coated fraction, a purity of 66% ± 8% could be reached, both at a yield above 57% (Figure 5b).

Accordingly, the general separability could be demonstrated on the basis of a surface coating of the PS particles reaching high purity. It should be noted that a sample volume of 1 µL was separated for each run of the experiments.

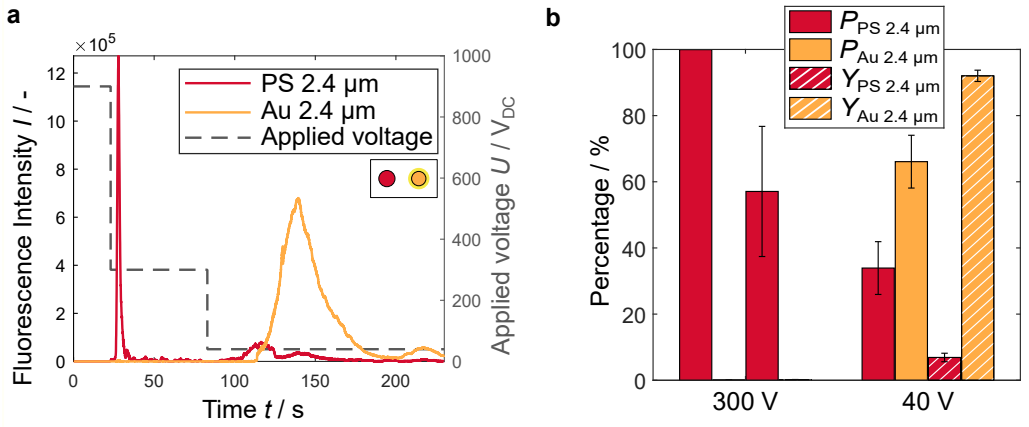

Figure 5. (**a**) Example dielectropherogram of a particle separation of 2.4 µm Au-coated and uncoated particles in DC-iEK microchannels (at pH 7.05, σ_m =29.5 µS cm^{-1}). The fluorescence intensity at the channel outlet is shown over the experimental period. The particles were trapped for several seconds at the inlet at highest voltage. With a voltage reduction, unmodified PS particles are released first, followed by smaller PS agglomerates and then gold-coated particles (based on [17]). (**b**) Corresponding calculated purity and yield of the separation process ($n = 3$).

3.2. Shape-Selective Separation

The separability of ellipsoidal and (treated) spherical particles of the same volume was shown in pressure-driven AC-iDEP microchannels as benchmark experiments (published in ref. [25]). Differences in Re$(\tilde{f}_{CM})$ due to the shape alteration were exploited. The aim was to show that both particles are retained with different trapping efficiencies. One particle shape is retained by strong pDEP, while the other type is retained less as it shows weak pDEP or nDEP. For the ellipsoids used in this experiments, a crossover of around 50 kHz was measured at a medium conductivity of $\sigma_m = 1.1$ µS cm^{-1}; for the spheres, a crossover of around 25 kHz was measured. At the chosen trapping frequency of 15 kHz, the Re$(\tilde{f}_{CM})$ factor for spherical particles is significant lower (Re$(\tilde{f}_{CM,sphere}) \approx 0.1$) than for ellipsoids of the same volume (Re$(\tilde{f}_{CM,ellipsoid}) \approx 0.5$) but is still positive. This results in an above 30% lower trapping efficiency for spherical compared to ellipsoidal particles (Figure 6a). The concentration of spheres (non-trapped) in the filtrate ("Sel. trapping" in Figure 6b) was increased from a purity of 50% to 68% ± 11%. After releasing the trapped particles ("Recovery" in Figure 6b), high purity was not reached for the ellipsoidal fraction, as no particle sample was separated in the preliminary experiments. Instead, the particle suspension was flushed through the channel for the entire experiment.

When evaluating the achieved purity, it must be considered that the stretching process leads to a distribution of the aspect ratio of the ellipsoids (see Appendix A Figure A1). Ellipsoids that were hardly deformed still behave more like spherical particles, but they are classified as ellipsoids due to their fluorescence color. Higher purities can therefore be expected if the actual aspect ratios of the separate fractions were considered. Compared to the material-based sorting, the separation based on the particle shape is more difficult due to smaller differences in Re$(\tilde{f}_{CM})$. It was therefore expected that lower purities would be achieved. Nevertheless, a different DEP behavior depending on the particle shape is evident, and a shape-based concentration is possible even at a volume flow of 0.1 mL h^{-1}.

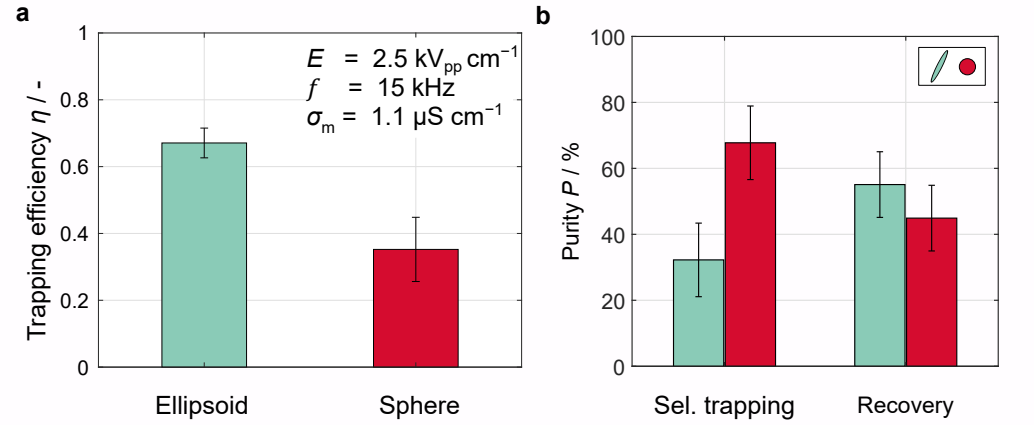

Figure 6. (**a**) Shape-selective trapping in AC-iDEP microchannels at $\sigma_m = 1.1$ µS cm^{-1} and a volume flow of $Q = 0.1$ mL h^{-1}. Trapping efficiency η was determined at a frequency of 15 kHz and an electric field of 2.5 kV$_{pp}$ cm^{-1} from a binary mixture of ellipsoids and treated spheres. Standard deviation is shown as error bars ($n = 3$). Adapted from ref. [25], published under CC BY 4.0 license. (**b**) Calculated purity of the filtrate for the selective trapping and remobilized fraction for the recovery step at the channel outlet.

3.3. Upscaling of AC-iDEP While Maintaining High Selectivity

In our previous publication [25], a prototype of a scalable DEP-filter was developed. With this filter, we were able to increase the volume flow by a factor of 1000 (0.1 mL h^{-1} vs. 120 mL h^{-1}) compared to our pressure-driven AC-iDEP microchannels. The functionality of the mesh-based DEP-filter was demonstrated by repeating the experiments from Section 3.2 (published in ref. [37]). Using comparable parameters (field strength, frequency and medium conductivity) and despite a 16 times higher superficial velocity in the insulating structures, higher trapping efficiencies for both particles were reached in the mesh-based filter ($\eta_{ellipsoids} = 94\% \pm 5\%$, $\eta_{spheres} = 51\% \pm 8\%$ [37] compared to $\eta_{ellipsoids} = 67\% \pm 5\%$, $\eta_{spheres} = 35\% \pm 10\%$ in the AC-iDEP microchannel, see Figure 6a). For the filtrate fraction, a purity of the ellipsoids of 74% ± 8% was achieved (Figure 7a) compared to 66% ± 11% in the AC-iDEP microchannel, which is in a similar range. One possible reason for the improved trapping efficiency of the macroscopic filter compared to the microchannel could be that the electrodes introduce the electric field over the entire channel length and perpendicular to the flow direction. Thus, the electric and velocity field maxima are not located at the same areas as it is the case in the AC-iDEP microchannels (see Figure 1).

After successfully verifying the general trapping performance, the mesh-based filter was investigated for its pDEP selectivity (published in ref. [26]). A prerequisite for complex sorting processes, such as the multidimensional sorting shown here, is high selectivity in terms of one type of trapping: in this case, pDEP. We compared the trapping efficiency at different medium conductivities where the PS particles changed from pDEP to nDEP with results of an irregular ceramic sponge that was used in ref. [23,36] (for a sketch, see Figure A2d). Similar trapping efficiencies were achieved for the medium conductivity range in which the particles exhibit pDEP (see Figure 7b). In the range for nDEP, the porous ceramic filter shows an increase in trapping efficiency to over 20%, whereas for the mesh-based filter, no nDEP trapping can be detected. Here, multidimensional sorting is based on releasing particles whose Re($\tilde{f}_{CM}$) is shifted towards nDEP. For this, nDEP retention in the filter is unfavorable. The increased pDEP selectivity of the regular filter structure can be attributed to the defined and regular spacing between the fibers (see Figure 1). In an irregular, porous structure, the particles are more likely to be exposed to lower field strengths within the individual pores, where they are also exposed to lower drag forces. In a regular mesh, on the other hand, a more uniform fluid velocity and thus also hardly any "dead zones" with combined field minima and low fluid velocity regions are expected.

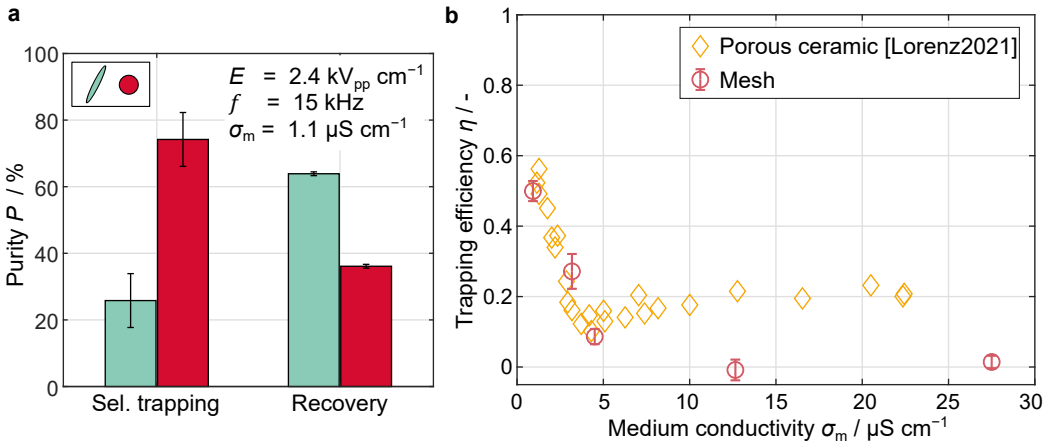

Figure 7. (**a**) Shape-selective trapping in a mesh-based DEP filter at $\sigma_m = 1.1$ µS cm^{-1} and a volume flow of $Q = 120$ mL h^{-1}. The purities for the selective trapping and recovery step were determined using a trapping frequency of 15 kHz and an electric field of 2.4 kV$_{pp}$ cm^{-1} from a binary mixture of ellipsoids and treated spheres. Standard deviation is shown as error bars ($n = 3$). (**b**) Comparison of the trapping efficiency over medium conductivity for trapping in a porous ceramic and mesh-based DEP filter. Experiments were done with spherical 4.5 µm PS particles at the same electric field strength $E = 1.1$ kV$_{pp}$ cm^{-1}, frequency $f = 15$ kHz, but different flow rates: 120 mL h^{-1} in the mesh-based ($n = 3$) and 240 mL h^{-1} in the ceramic filter with a hydraulic diameter of 222 µm. The data for the porous ceramic filter were extracted from ref. [36] ([Lorenz2021] in figure legend). The electrodes of the mesh filter had a distance of 0.7 mm. Adapted from ref. [26], published under CC BY 4.0 license.

3.4. Multidimensional Sorting

The previous sections have shown that the individual particle modifications are suitable to create a model particle system which is separable with (standard) DEP methods. Furthermore, it was proven that the new high-throughput DEP filter with regular structures has both sufficiently high trapping efficiencies and higher pDEP selectivity than previous DEP filters with irregular structures. The prerequisites for testing multidimensional separation according to the concept described in Section 2.3 were thus fulfilled.

During the project, the individual steps for a multidimensional sorting process (selective trapping and selective remobilization) were initially examined separately. First, selective trapping in DEP filters was investigated (see Section 3.3), followed by selective remobilization (ref. [25]). For selective remobilization, all particle types were first retained in the filter structure and subsequently selectively remobilized by a shift of the trapping frequency. The influence of the dielectrophoretic particle properties and the remobilization frequency were investigated (ref. [25]). After successful implementation in the mesh-based DEP filter, the steps were combined into an multi-step sorting process (Figure 4, published in ref. [26]) and summarized in the following paragraph.

A mixture of two different-sized spherical PS particles (treated, 2.5 µm and 5 µm), as well as 3 µm gold-coated PS particles and originally 2.5 µm ellipsoidal particles, was sorted. The slightly larger Au-coated particles were chosen to make it easier to distinguish the particles on SEM images. At a frequency of 30 kHz, all particle types but the large spherical particles were retained in the filter with a trapping efficiency of over 75% (Figure 8a). In the filtrate, the 5 µm particles were enriched to a purity of 67% (Figure 8b) as they are the only particle type that show nDEP. Afterward, the particle suspension was replaced by a flushing solution, resulting in a decrease in fluorescence intensity for all particle types. Subsequently, the frequency was increased in two steps. The frequencies were chosen in such a way that for each increase the crossover of only one particle type was passed (see Figure 4b). The first step (77 kHz) released the small spherical particles, the second step (150 kHz) mainly comprised ellipsoidal particles. Both fractions reached a purity of above 65% (Figure 8b). No gold-coated particles were released during the remobilization steps, as they show pDEP at all applied frequencies. Therefore, a high yield was reached

for the gold-coated fraction in the recovery steps when the electric field was switched off (Figure 8c). However, a purity of 55% was lower compared to the other particles because some particles of the other types could only be released when switching off the electric field. We assume other (electrokinetic) forces to be responsible for the remaining retention of PS particles (especially the spherical ones) as nDEP trapping was excluded. The exact cause could not be identified, but the fact that the particles are released after the voltage is switched off supports the theory of an electrokinetic effect. A clear enrichment of each particle type in the specific fraction was achieved in the multidimensional sorting process. Example SEM images of the collected samples can be found in the Appendix A (Figure A4). As the properties of the particles are distributed after the modification steps (PVA amount left on the surface, aspect ratio of the ellipsoids, or gold-coating thickness), the dielectric properties are distributed as well, which results in overlapping DEP behavior and purities below 70%. Nevertheless, despite the more complex separation task and a 1000 times higher volume flow, similar purities could be reached compared to the shape-based separation in AC-iDEP microchannels.

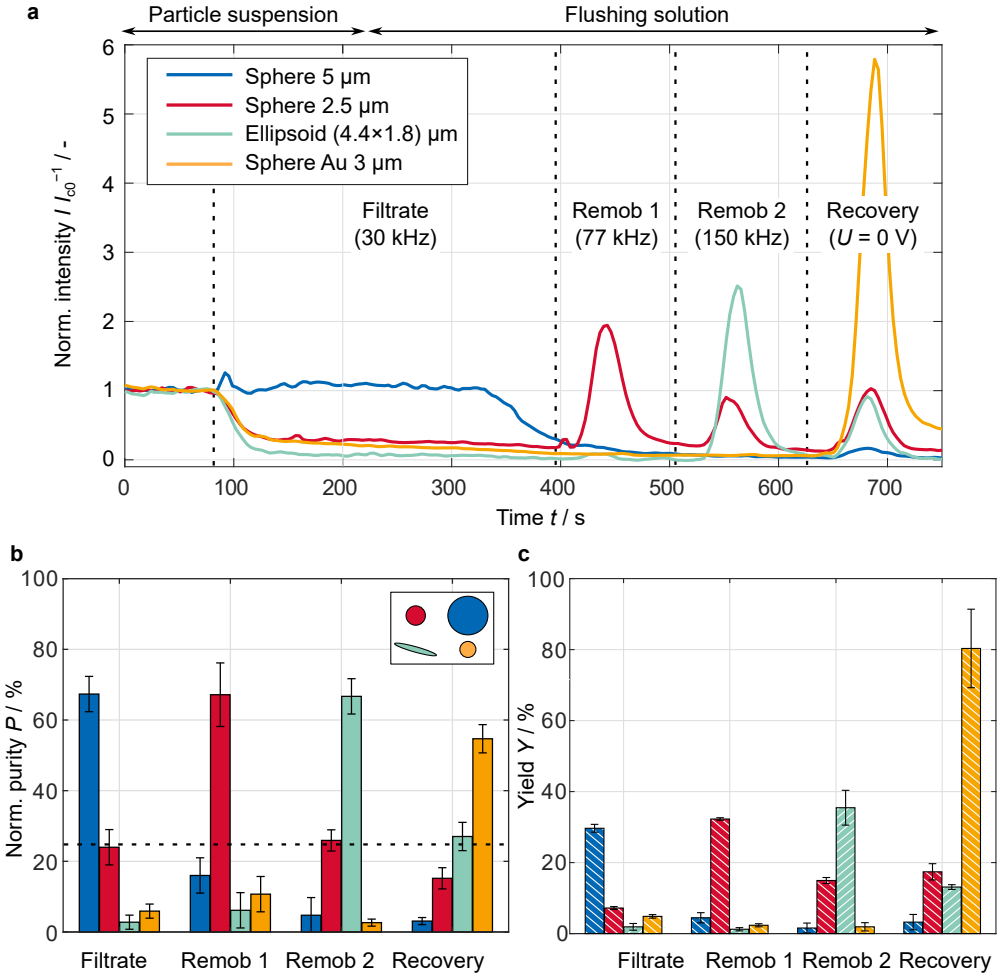

Figure 8. Multi-step sorting process at $Q = 120$ mL h^{-1}, $\sigma_m = 1.5$ µS cm^{-1}, and $E = 2.9$ kV$_{pp}$ cm^{-1} (at 0.9 mm electrode distance). Adapted from ref. [26], published under CC BY 4.0 license. (**a**) Mean normalized fluorescence intensity over experimental time. Data were determined with only one particle type in the suspension ($n = 3$). The dashed lines delimit the given process step names. (**b**) Normalized purity before (dashed line) and after the sorting process. A particle mixture was used, and samples of each fraction were collected ($n = 3$). Here, the standard deviation for the evaluation of multiple SEM images is given instead of the standard deviation for the experimental replicates. (**c**) Yielddetermined for the same time intervals as the sample collection, but from experiments with only one type of particle present in the suspension ($n = 3$).

An improvement of the sorting can probably be achieved by using more powerful amplifiers with a higher slew rate. The maximum remobilization frequency of the used amplifier is not sufficient for shifting strongly elongated ellipsoids to nDEP. Therefore, some of these particles end up in the recovery fraction. In addition, increasing the time between switching to the flushing solution and the first remobilization step could improve the purity of the first remobilization fraction. Remobilization at a slightly higher flow rate can increase the remobilization rate of particles exhibiting nDEP, which are likely trapped by other forces except DEP. This is also an option to concentrate the particles in comparison to the original particle concentration of the suspension.

4. Conclusions and Outlook

As part of this project, an operation mode for DEP filters was developed to sort microparticle mixtures based on several properties. This was demonstrated using polystyrene microparticles, which were sorted based on their size, shape, and surface coating. It was exploited that the relative particle polarization depends on the particle properties and the frequency of the electric field. This means that the direction of the DEP force and which particles are retained in the DEP filter can be changed, simply by switching the frequency of the applied electric field. At the same time, a scalable approach for DEP filters was developed that enables an increase in throughput while maintaining the high selectivity of microfluidic DEP setups. Regular filter structures in the form of meshes were used for this. In sorting the model system used in this project, the mesh-based DEP filter performed similarly to the more common microchannel designs (DC-iEK, AC-iDEP) tested in this project. Compared to high-throughput devices with irregular filter structures, this approach offers the advantage that lower voltages can be used and a higher selectivity for pDEP trapping can be achieved. The particle system developed as part of this project, especially the ellipsoidal particles, was also used by other groups of the priority program (e.g., [38]) and made it possible to specifically investigate the particle shape without changing the particle material or volume at the same time. We used microparticles here to make them easier to observe online and to create a range of particle types, each of which differs from the other types in only one aspect. However, the results should be transferable to smaller particles. It should be possible to change the filter material and mesh size to adapt the filter to different particle systems. These parameters need to be investigated in the future to determine their influence on the DEP force and pressure drop across the filter.

Further upscaling of the mesh-based DEP filter can be realized in two different ways: we can increase the filters' cross-section in width and we can stack multiple filter units. The decisive factor is that both methods preserve the positive characteristic of microfluidic devices, namely a small electrode gap. An increase in the spacing requires higher voltages to be applied in order to generate a sufficient field strength for DEP and result in longer distances for the particles to travel to trapping spots. Furthermore, at low voltages, the range for setting the frequency, which can be used to achieve the crossover of individual particles, is larger. This is because the primary reason for the frequency limitation of DEP setups lies in the maximum possible slew rate ($\mathrm{d}U/\mathrm{d}t$) of the amplifier. A large frequency range is a fundamental requirement of multidimensional sorting, as proposed in this project. However, a limitation of the maximum possible size of a DEP filter is a limited output current supply of amplifiers. The current flow increases with an increasing electrode surface. The use of more powerful amplifiers can possibly significantly increase the maximum size and therefore the maximum throughput. The limits of scaling with respect to thermal management and power supply require further research. Apart from this, throughput can be increased by an interconnection to a semi-continuous sorting process, as shown in a cooperation project [39]. In that concept, two pumps and an automatic valve switching system were used to alternately feed two DEP setups in parallel with a flushing solution and the particle mixture. This can be transferred accordingly to the method shown in this project, thus offering the possibility to sort microparticles cost- and time-effectively.

One major drawback of the selective remobilization concept, however, is that the change in direction of the DEP force is not achievable or not yet realizable for all materials. For semiconducting materials, in particular, the crossover frequencies are in a range that is theoretically achievable (MHz). Research is needed on how the MHz frequency area can be reached with scalable DEP setups and commercially available amplifier technology. Initial steps to extend the frequency range of high-throughput DEP devices have been taken in our group at the example of a different DEP setup [40]. However, both further upscaling and the extension of the frequency range need to be investigated more extensively in order to make DEP attractive for a wide range of technical applications.

In summary, the results of this project (DFG project number 382080004) contribute to the understanding of multidimensional sorting using dielectrophoresis and show a way to process non-biological particles by enabling the scalability of DEP methods. Therefore, this study contributes to the overall goal of the SPP 2045 to develop future technologies that pave the way for the efficient production of ultra-fine highly specific particle systems.

Author Contributions: Conceptualization, J.T. and L.W.; methodology, all authors; software, J.G. and L.W.; data curation, L.W.; writing—original draft preparation, L.W.; writing—review and editing, all authors; visualization, L.W.; supervision, J.T.; project administration, M.B., G.R.P. and J.T.; funding acquisition, M.B., G.R.P. and J.T. All authors have read and agreed to the published version of the manuscript.

Funding: This project was funded by the German Research Foundation (DFG) within the priority program, "MehrDimPart—Highly specific and multidimensional fractionation of fine particle systems with technical relevance" (SPP2045, grant numbers TH 893/20-1 and TH 893/20-2). Contributions from cooperating SPP projects were funded under grant numbers BA 1893/2-1 (J.G. and M.B.) and PE 3015/3-2 (J.G. and G.R.P.).

Institutional Review Board Statement: Not applicable.

Informed Consent Statement: Not applicable.

Data Availability Statement: All measurement data, evaluation and visualization scripts of refs. [25,26] can be found separately for the individual publications in online repositories [41,42]. Data of ref. [17] is available from the authors upon reasonable request.

Conflicts of Interest: The authors declare no conflicts of interest.

Abbreviations

The following abbreviations are used in this manuscript:

AC	Alternating current
CM	Clausius–Mossotti
DC	Direct current
DEP	Dielectrophoresis
EK	Electrokinetic
EO	Electro-osmosis
EP	Electrophoresis
iDEP	Insulator-based dielectrophoresis
ITO	Indium tin oxide
nDEP	Negative dielectrophoresis
pDEP	Positive dielectrophoresis
PDMS	Polydimethylsiloxane
pp	Peak-to-peak
PP	Polypropylene
PS	Polystyrene
PVA	Polyvinyl alcohol
SEM	Scanning electron microscope

Appendix A

Appendix A.1. Equations Used for the Calculation of Separation Parameters

Both trapping efficiency and yield were determined from fluorescence intensity signals. It was assumed that the fluorescence intensity depends linearly on the number of particles flowing through the flow-through cuvette in the concentration range used. The trapping efficiency

$$\eta = 1 - \frac{\bar{I}_{\mathrm{DEP}}}{\bar{I}_{\mathrm{c0}}} \tag{A1}$$

was calculated as a mean signal reduction between the initial signal $\bar{I}_{\mathrm{c0}}$ and the signal during trapping $\bar{I}_{\mathrm{DEP}}$.

The yield of one species a characterizes how large the proportion of the collected particle quantity is compared to the total quantity of processed particles of this type

$$Y_a = \frac{N_{a,\mathrm{out}}}{N_{a,\mathrm{in}}} = \frac{\int I_a dt}{\bar{I}_{a,c_0} t_{\mathrm{solution,change}}} \,. \tag{A2}$$

The processed particle quantity $N_{a,\mathrm{in}}$, in the case of multidimensional experiments, was determined up to the time of the change to a flushing solution ($t_{\mathrm{solution,change}}$). The collected particle quantity $N_{a,\mathrm{out}}$ was calculated by integrating the fluorescence signal over the time period during which the sample is collected.

The purity P

$$P_a = \frac{N_a}{N_a + N_b} \tag{A3}$$

was determined with N_b being the number of all other particles types, except type a, in the collected fraction. For the multidimensional experiments, the purity was determined from SEM image samples of the collected fraction. In order to evaluate the sorting performance independently of any initial concentration original particle mixture's differences; here, all particle numbers were normalized to their total/initial number.

Appendix A.2. Additional Figures

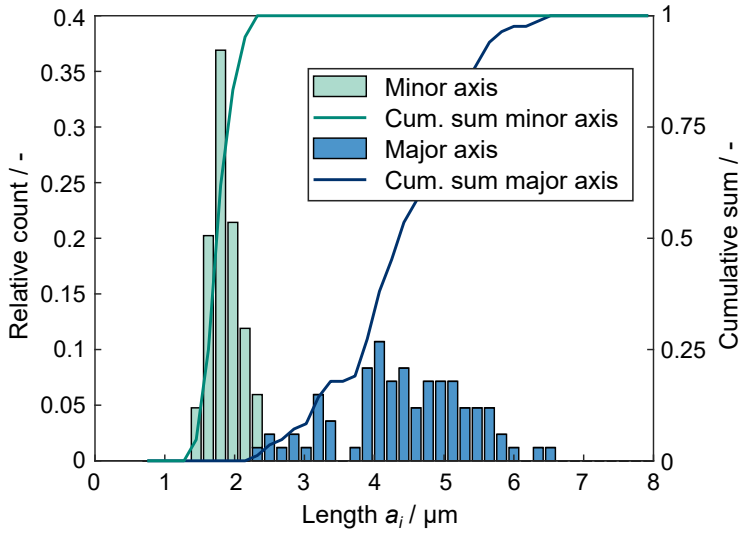

Figure A1. Distribution and cumulative sum of the diameters a_i of an example ellipsoid batch after the stretching process (used for the multidimensional sorting experiments). Published in ref. [26] under CC BY 4.0 license.

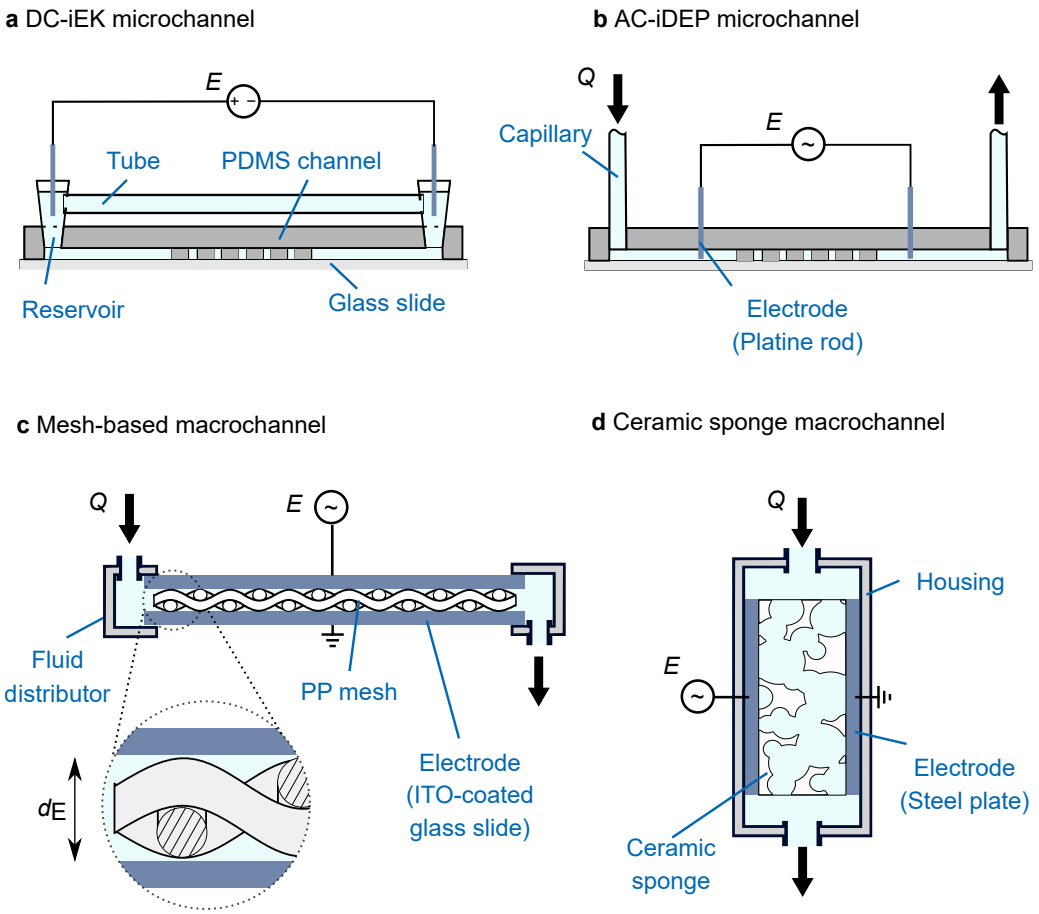

Figure A2. Sketch of the DEP channel types used in this work (not for scale). (**a**) DC-iEK microchannel. Based on [17]. (**b**) AC-iDEP microchannel. (**c**) Mesh-based macrochannel. Based on [25]. (**d**) Ceramic sponge macrochannel.

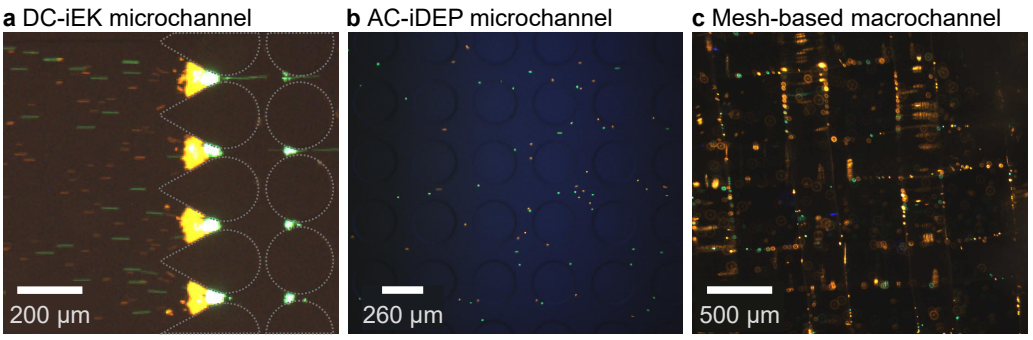

Figure A3. Fluorescence microscope images from the different DEP filter types used in this project. The direction of flow occurs from left to right in each case. (**a**) DC-iEK microchannel. Based on [17] with highlighted post outlines for better visibility. Particles are retained in front of the post array structure. (**b**) AC-iDEP microchannel. Particles are trapped at the edges of the posts. (**c**) Mesh-based macrochannel. Particles are trapped at the edges of the mesh fibers.

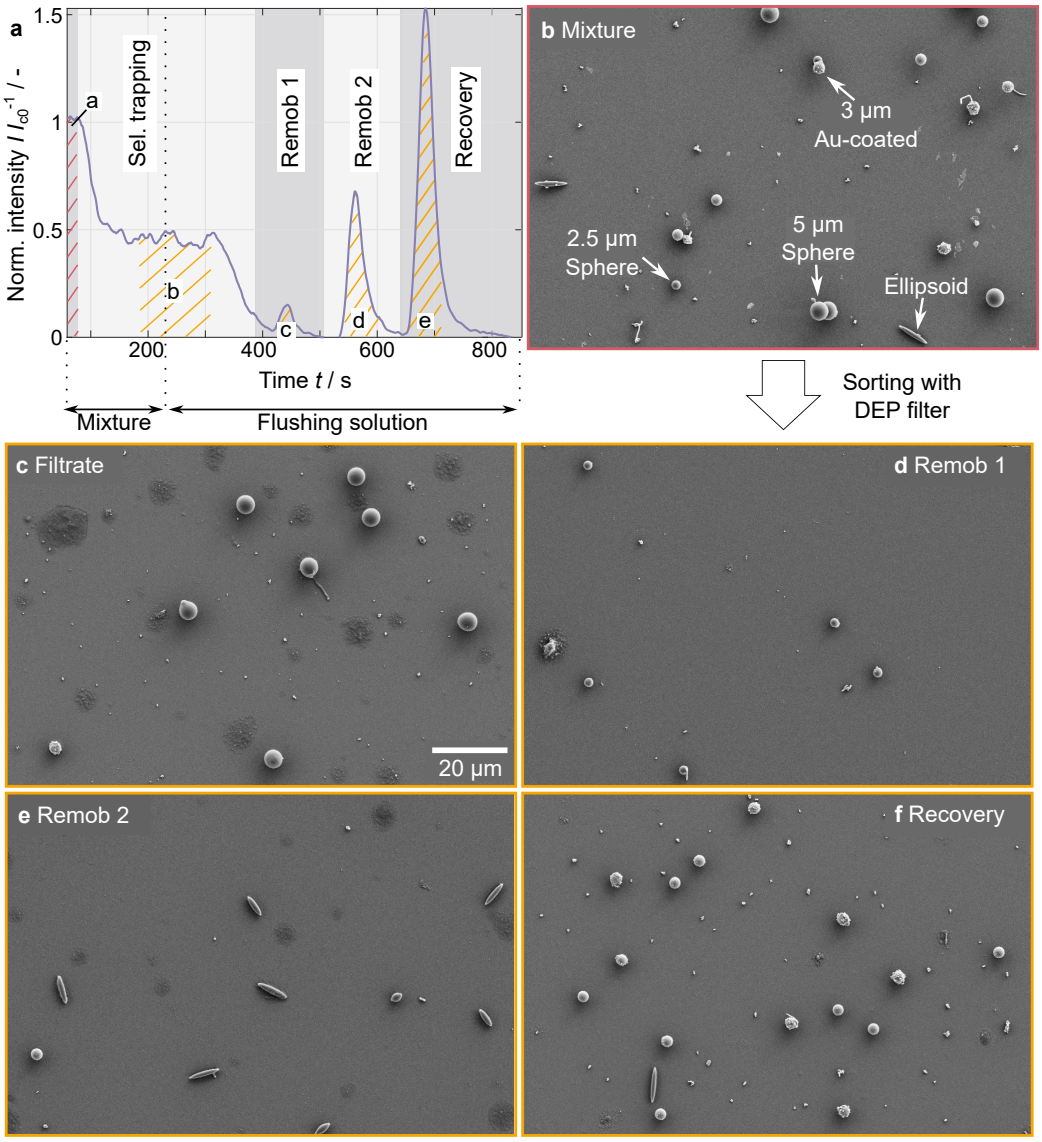

Figure A4. Example SEM images of the collected fractions ($Q = 120$ mL h^{-1}, $\sigma_m = 1.5$ µS cm^{-1}, $E = 2.9$ kV$_{pp}$ cm^{-1} at 0.9 mm electrode distance). For data determination (purity), a lower magnification factor and several images were used for each collected fraction. Published in ref. [26] under CC BY 4.0 license. (**a**) Sampling intervals for an experiment shown at the normalized, total intensity (not divided into different fluorescence colors). The letters link the indicated sample collection times (hatched areas) to the SEM images with correspondingly colored frames (red: mixture, yellow: after sorting). (**b**) Particle suspension before sorting (mixture) containing spherical particles of two sizes (2.5 µm and 5 µm), ellipsoids (same volume as 2.5 µm sphere), and gold-coated particles (3 µm). (**c**–**f**) Single fractions after sorting.

References

1. Presser, V.; Dennison, C.R.; Campos, J.; Knehr, K.W.; Kumbur, E.C.; Gogotsi, Y. The Electrochemical Flow Capacitor: A New Concept for Rapid Energy Storage and Recovery. *Adv. Energy Mater.* **2012**, *2*, 895–902. [CrossRef]
2. Rabbani, M.T.; Schmidt, C.F.; Ros, A. Single-Walled Carbon Nanotubes Probed with Insulator-Based Dielectrophoresis. *Anal. Chem.* **2017**, *89*, 13235–13244. [CrossRef] [PubMed]
3. Behdani, B.; Monjezi, S.; Carey, M.J.; Weldon, C.G.; Zhang, J.; Wang, C.; Park, J. Shape-Based Separation of Micro-/Nanoparticles in Liquid Phases. *Biomicrofluidics* **2018**, *12*, 051503. [CrossRef] [PubMed]
4. Buchwald, T.; Ditscherlein, R.; Peuker, U.A. Beschreibung von Trennoperationen mit mehrdimensionalen Partikeleigenschaftsverteilungen. *Chem. Ing. Tech.* **2023**, *95*, 199–209. [CrossRef]
5. Wu, Y.; Chattaraj, R.; Ren, Y.; Jiang, H.; Lee, D. Label-Free Multitarget Separation of Particles and Cells under Flow Using Acoustic, Electrophoretic, and Hydrodynamic Forces. *Anal. Chem.* **2021**, *93*, 7635–7646. [CrossRef]

6. Pohl, H.A.; Pollock, K.; Crane, J.S. Dielectrophoretic Force: A Comparison of Theory and Experiment. *J. Biol. Phys.* **1978**, *6*, 133–160. [CrossRef]
7. Kirby, B.J. *Micro- and Nanoscale Fluid Mechanics: Transport in Microfluidic Devices*; Cambridge University Press: New York, NY, USA, 2010.
8. Pethig, R. *Dielectrophoresis: Theory, Methodology, and Biological Applications*; John Wiley & Sons, Inc.: Hoboken, NJ, USA, 2017.
9. O'Konski, C.T. ELECTRIC PROPERTIES OF MACROMOLECULES. V. THEORY OF IONIC POLARIZATION IN POLYELECTROLYTES. *J. Phys. Chem.* **1960**, *64*, 605–619. [CrossRef]
10. Green, N.G.; Morgan, H. Dielectrophoresis of Submicrometer Latex Spheres. 1. Experimental Results. *J. Phys. Chem. B* **1999**, *103*, 41–50. [CrossRef]
11. Ermolina, I.; Morgan, H. The Electrokinetic Properties of Latex Particles: Comparison of Electrophoresis and Dielectrophoresis. *J. Colloid Interface Sci.* **2005**, *285*, 419–428. [CrossRef]
12. Jen, C.P.; Chen, T.W. Selective Trapping of Live and Dead Mammalian Cells Using Insulator-Based Dielectrophoresis within Open-Top Microstructures. *Biomed. Microdevices* **2009**, *11*, 597–607. [CrossRef]
13. Suehiro, J.; Zhou, G.; Imamura, M.; Hara, M. Dielectrophoretic Filter for Separation and Recovery of Biological Cells in Water. *IEEE Trans. Ind. Appl.* **2003**, *39*, 1514–1521. [CrossRef]
14. Kepper, M.; Rother, A.; Thöming, J.; Pesch, G.R. Polarisability-Dependent Separation of Lithium Iron Phosphate (LFP) and Graphite in Dielectrophoretic Filtration. *Results Eng.* **2024**, *21*, 101854. [CrossRef]
15. Lapizco-Encinas, B.H.; Simmons, B.A.; Cummings, E.B.; Fintschenko, Y. Insulator-Based Dielectrophoresis for the Selective Concentration and Separation of Live Bacteria in Water. *Electrophoresis* **2004**, *25*, 1695–1704. [CrossRef] [PubMed]
16. Moncada-Hernández, H.; Lapizco-Encinas, B.H. Simultaneous Concentration and Separation of Microorganisms: Insulator-Based Dielectrophoretic Approach. *Anal. Bioanal. Chem.* **2010**, *396*, 1805–1816. [CrossRef] [PubMed]
17. Weirauch, L.; Lorenz, M.; Hill, N.; Lapizco-Encinas, B.H.; Baune, M.; Pesch, G.R.; Thöming, J. Material-Selective Separation of Mixed Microparticles via Insulator-Based Dielectrophoresis. *Biomicrofluidics* **2019**, *13*, 064112. [CrossRef]
18. Pethig, R. Review Article—Dielectrophoresis: Status of the Theory, Technology, and Applications. *Biomicrofluidics* **2010**, *4*, 022811. [CrossRef]
19. Martinez-Duarte, R. A Critical Review on the Fabrication Techniques That Can Enable Higher Throughput in Dielectrophoresis Devices. *Electrophoresis* **2022**, *43*, 232–248. [CrossRef]
20. Oberton, S.B. Electrofiltration Process for Purifying Organic Liquids. U.S. Patent 4040926, 9 August 1977.
21. Crissman, J.H.; Fritsche, R.G.; Hamel, F.B.; Hilty, L.W. Radial Flow Electrostatic Filter. U.S. Patent 4059498, 22 November 1977.
22. Pesch, G.R.; Lorenz, M.; Sachdev, S.; Salameh, S.; Du, F.; Baune, M.; Boukany, P.E.; Thöming, J. Bridging the Scales in High-Throughput Dielectrophoretic (Bio-)Particle Separation in Porous Media. *Sci. Rep.* **2018**, *8*, 10480. [CrossRef]
23. Lorenz, M.; Malangré, D.; Du, F.; Baune, M.; Thöming, J.; Pesch, G.R. High-Throughput Dielectrophoretic Filtration of Sub-Micron and Micro Particles in Macroscopic Porous Materials. *Anal. Bioanal. Chem.* **2020**, *412*, 3903–3914. [CrossRef]
24. Pesch, G.R.; Du, F. A Review of Dielectrophoretic Separation and Classification of Non-biological Particles. *Electrophoresis* **2021**, *42*, 134–152. [CrossRef]
25. Weirauch, L.; Giesler, J.; Baune, M.; Pesch, G.R.; Thöming, J. Shape-Selective Remobilization of Microparticles in a Mesh-Based DEP Filter at High Throughput. *Sep. Purif. Technol.* **2022**, *300*, 121792. [CrossRef]
26. Weirauch, L.; Giesler, J.; Pesch, G.R.; Baune, M.; Thöming, J. Sorting Microparticle Mixtures by Multiple Properties in a Single Dielectrophoretic Filter. *Results Eng.* **2024**, *23*, 102641. [CrossRef]
27. Barua, S.; Yoo, J.W.; Kolhar, P.; Wakankar, A.; Gokarn, Y.R.; Mitragotri, S. Particle Shape Enhances Specificity of Antibody-Displaying Nanoparticles. *Proc. Natl. Acad. Sci. USA* **2013**, *110*, 3270–3275. [CrossRef] [PubMed]
28. Lim, J.K.; Eggeman, A.; Lanni, F.; Tilton, R.D.; Majetich, S.A. Synthesis and Single-Particle Optical Detection of Low-Polydispersity Plasmonic-Superparamagnetic Nanoparticles. *Adv. Mater.* **2008**, *20*, 1721–1726. [CrossRef]
29. Ren, Y.K.; Morganti, D.; Jiang, H.Y.; Ramos, A.; Morgan, H. Electrorotation of Metallic Microspheres. *Langmuir ACS J. Surfaces Colloids* **2011**, *27*, 2128–2131. [CrossRef]
30. García-Sánchez, P.; Ren, Y.; Arcenegui, J.J.; Morgan, H.; Ramos, A. Alternating Current Electrokinetic Properties of Gold-Coated Microspheres. *Langmuir* **2012**, *28*, 13861–13870. [CrossRef]
31. Ho, C.C.; Keller, A.; Odell, J.A.; Ottewill, R.H. Preparation of Monodisperse Ellipsoidal Polystyrene Particles. *Colloid Polym. Sci.* **1993**, *271*, 469–479. [CrossRef]
32. Moncada-Hernandez, H.; Baylon-Cardiel, J.L.; Pérez-González, V.H.; Lapizco-Encinas, B.H. Insulator-Based Dielectrophoresis of Microorganisms: Theoretical and Experimental Results. *Electrophoresis* **2011**, *32*, 2502–2511. [CrossRef]
33. Saucedo-Espinosa, M.A.; Lapizco-Encinas, B.H. Experimental and Theoretical Study of Dielectrophoretic Particle Trapping in Arrays of Insulating Structures: Effect of Particle Size and Shape: Microfluidics and Miniaturization. *Electrophoresis* **2015**, *36*, 1086–1097. [CrossRef]
34. Srivastava, S.K.; Gencoglu, A.; Minerick, A.R. DC Insulator Dielectrophoretic Applications in Microdevice Technology: A Review. *Anal. Bioanal. Chem.* **2011**, *399*, 301–321. [CrossRef]
35. Lapizco-Encinas, B.H. The Latest Advances on Nonlinear Insulator-Based Electrokinetic Microsystems under Direct Current and Low-Frequency Alternating Current Fields: A Review. *Anal. Bioanal. Chem.* **2022**, *414*, 885–905. [CrossRef] [PubMed]

36. Lorenz, M. Dielectrophoretic Filtration of Particles in Porous Media: Concept, Design, and Selectivity. Ph.D. Thesis, Universität Bremen, Bremen, Germany, 2021. [CrossRef]
37. Weirauch, L. Multidimensional Sorting of Microparticles in Electrically Switchable Dielectrophoretic Filters. Ph.D. Thesis, Universität Bremen, Bremen, Germany, 2023. [CrossRef]
38. Sachs, S.; Schmidt, H.; Cierpka, C.; König, J. On the Behavior of Prolate Spheroids in a Standing Surface Acoustic Wave Field. *Microfluid. Nanofluid.* **2023**, *27*, 81. [CrossRef]
39. Giesler, J.; Weirauch, L.; Pesch, G.R.; Baune, M.; Thöming, J. Semi-Continuous Dielectrophoretic Separation at High Throughput Using Printed Circuit Boards. *Sci. Rep.* **2023**, *13*, 20696. [CrossRef] [PubMed]
40. Giesler, J.; Weirauch, L.; Thöming, J.; Baune, M. Compensation of Capacitive Currents in High-Throughput Dielectrophoretic Separators. *Sci. Rep.* **2024**, *14*, 16491. [CrossRef]
41. Weirauch, L. Repository for 'Shape-selective Remobilization of Microparticles in a Mesh-Based DEP Filter at High Throughput'. 2022. Available online: https://zenodo.org/records/6534451 (accessed on 28 August 2024).
42. Weirauch, L. Online Repository for: "Sorting Microparticle Mixtures by Multiple Properties in a Single Dielectrophoretic Filter". 2023. Available online: https://zenodo.org/records/10303592 (accessed on 28 August 2024).